Available online at www.sciencedirect.com
SCIENCE DIRECT®
Proceedings of the Combustion Institute 30 (2005) 809–817
Proceedings of the Combustion Institute
www.elsevier.com/locate/proci

Curvature and wrinkling of premixed flame kernels—comparisons of OH PLIF and DNS data

Sara Gashi[a,c,*], Johan Hult[b], Karl W. Jenkins[c], Nilanjan Chakraborty[c], Stewart Cant[c], Clemens F. Kaminski[a,*]

[a] *Department of Chemical Engineering, University of Cambridge, Pembroke Street, Cambridge CB2 3RA, UK*
[b] *Department of Combustion Physics, Lund Institute of Technology, P.O. Box 118, SE-22100 Lund, Sweden*
[c] *Department of Engineering, University of Cambridge, Trumpington Street, Cambridge CB2 1PZ, UK*

Abstract

The effects of curvature and wrinkling on the growth of turbulent premixed flame kernels have been investigated using both 2D OH planar laser-induced fluorescence (PLIF) and 3D direct numerical simulation (DNS). Comparisons of results between the two approaches show a high level of agreement, providing confidence in the simplified chemistry treatment employed in the DNS, and indicating that chemistry may have only a limited influence on the evolution of the freely propagating flame. This is in contrast to previous studies of the very early flame development where chemistry may be dominant. Statistics for curvature and wrinkling are presented in the form of probability density functions, and there is good agreement with previous findings. The limitations of 2D PLIF measurements of curvature are quantified by comparison with full 3D information obtained from the DNS. The usefulness of PLIF in providing data over a wide parameter range is illustrated using statistics obtained from both CH_4/air and H_2/air mixtures, which show a markedly different behaviour due to their different thermo-diffusive properties. The results provide a demonstration of the combined power of PLIF and DNS for flame investigation. Each technique is shown to compensate for the weaknesses of the other and to reinforce the strengths of both.

Keywords: Turbulent premixed; PLIF; DNS

1. Introduction

Turbulent premixed flame propagation is known to strongly depend on the degree of wrinkling of the flame surface [1] and its effect on the total surface area available for reaction. Overall flame wrinkling is closely related to flame curvature, but the direct effects of local curvature on flame propagation have been found to be relatively weak [2,3] for flames at near-unity Lewis number and well within the wrinkled or corrugated flamelet regime [4]. This is due to a rough balance between positive and negative curvature throughout the flame, and to the existence of a roughly linear relationship between the local burning rate and the modest values of curvature that are encountered [5]. Theoretical predictions [6] for flames within the thin reaction zone regime suggest that the dependence on curvature is rather stronger in this regime, and this has been borne

* Corresponding authors. Fax: +44 0 1223 334 796 (S. Gashi), +44 0 1223 334 796 (C.F. Kaminski).
E-mail addresses: sg341@eng.cam.ac.uk (S. Gashi), clemens_kaminski@cheng.cam.ac.uk (C.F. Kaminski).

1540-7489/$ - see front matter
doi:10.1016/j.proci.2004.08.003

out by experiment [7] and direct numerical simulation (DNS) [8,9]. The dependence of displacement speed on curvature is of particular interest in the modelling of premixed flame propagation for both large-Eddy simulation (LES) and Reynolds averaged Navier–Stokes (RANS) approaches.

The flame kernel configuration offers a number of advantages for the study of flame curvature in the thin reaction zone regime. There is an obvious and direct application to spark-ignition engine combustion. From the experimental standpoint, the turbulence can be made homogeneous and isotropic to a high degree, and high values of the turbulent velocity fluctuation magnitude can be attained together with well-controlled turbulent length scales [10–13]. From the computational standpoint, the problem is greatly simplified by the absence of mean flow, there is no need to provide a mechanism for flame stabilisation, and the flame remains far from walls or other obstructions for which geometrical details and boundary conditions would have to be supplied. Previous experimental results have characterised flame kernel growth during early times after ignition, based on 2D planar laser-induced fluorescence (PLIF) images [12,14], while previous DNS has provided both 2D [15] and 3D curvature statistics [16,17]. A previous comparison between 3D experiment and LES [18] showed good agreement using the particular sub-grid model in question [19].

The purpose of the present work was to make a direct comparison between curvature statistics obtained from both experiment and DNS, and to evaluate the effects of wrinkling on the properties of turbulent premixed flame kernels. Data have been obtained both from full 3D DNS calculations with single step chemistry at low to moderate turbulence intensities, and from time-resolved PLIF measurements under similar conditions using spark ignited mixtures subjected to variable and controlled degrees of turbulence. The conditions for both DNS and experiment are similar: u'/S_L range from 0 to 10 in both cases. Experiments were performed for l_t/δ_l ranging from 0 to 50, and calculations for l_t/δ_l between 0 and 20. Thus, the turbulence Reynolds number Re_t is comparable between simulations and experiments. Probability density functions (pdfs) for flame curvature have been obtained on the PLIF data and on 2D slices from the calculated DNS flame kernels for different levels of turbulence. Qualitatively the two are in excellent agreement.

2. Experimental details

2.1. Combustion bomb

The combustion cell and ignition system designed at the Institute for Combustion Technology, University of Stuttgart, were used in the present experiments. The set-up and details of the facility have been described in detail in previous applications [12,21,22]. Briefly, two electrodes, separated by 1 mm, in the centre of the cell were used to ignite the premixed fuel/air mixtures. The cell was equipped with four rotors used to control the turbulence intensity imparted to the flame. Levels of turbulence intensities imparted on the mixtures could be controlled precisely by varying the rotor speeds. The turbulence field was characterised in detail in previously performed LDV measurements [21] for each corresponding rotor speed and was found to be isotropic in all cases. Rotor speeds were varied from 1000 to 3000 rpm ($u'/S_L = 1.62$–$u'/S_L = 5.25$) for the CH_4/air mixtures, and 1000 to 5000 rpm ($u'/S_L = 0.41$–$u'/S_L = 2.21$) for H_2/air mixtures. Integral length scales are estimated to be of order 7 mm. The spark ignition system was designed to deliver precisely controllable amounts of energy into the mixture and has also been characterised in detail [14].

2.2. PLIF measurements

Time sequences of OH distributions in the flame kernels were recorded using the high-speed imaging facility at the Lund Institute of Technology. Details of the system and the set-up used for OH spectroscopy have been described in previous publications [14,20].

Briefly, a cluster of four Nd:YAG lasers was fired sequentially at high repetition rates and used to pump a dye laser. The frequency doubled dye laser beam was formed into a sheet of 40 mm in height and approximately 300 μm in width using a cylindrical telescope. The fluorescence signals were collected at right angles by a high-speed camera consisting of 8 independent ICCD (intensified CCD) detectors (384×576 pixels and 8 bit dynamic resolution). Individual events were imaged onto different ICCDs by use of a pyramid beam-splitter inside the camera. Recording rates of up to 1 MHz are possible with this system by sequential gating of individual ICCDs. OH was excited using the temperature insensitive $Q_1(8)$ transition in the $A^2\Sigma^+(v' = 1) \leftarrow X^2\Pi(v'' = 0)$ electronic band, which corresponds to a wavelength near 283.5 nm. The resulting fluorescence was collected in the $v' = 0 \rightarrow v'' = 0$ and $v' = 1 \rightarrow v'' = 1$ bands around 310 nm.

3. Computational details

Simulations were performed using the SENGA DNS code, developed at the University of Cambridge, which is based on the solution of the compressible Navier–Stokes, species and energy equations for a lean hydrocarbon mixture. The explicit finite difference algorithm uses a 10th order

scheme for spatial differencing and a low storage 3rd order Runge–Kutta method for time stepping. Boundary conditions were treated using the NSCBC (Navier–Stokes Characteristic Boundary Condition) formulation [23]. The wall boundaries are far enough from the flame, so that the flow properties will not be affected. The 3D flame kernel evolution in the turbulent field was considered to be of primary importance, therefore chemistry was simplified to a single step reaction following Arrhenius kinetics. A major goal of the current research was to test the validity of this simplification by comparing the statistical properties of the evolving flame kernels with experiments. A single reaction progress variable, c, was used to describe the chemical state of the mixture, varying from zero in the fresh gases to one for the fully burned mixture. Two different domain sizes were considered, containing 96^3 and 128^3 grid points. These correspond to maximum turbulent Reynolds numbers of 20 and 30, respectively. Computations were initialised by a pre-computed laminar flame kernel that is allowed to evolve a short time before beginning to interact with the turbulent field of different intensities u'/S_L. To facilitate a direct comparison with the experimental data, which is 2D in nature, 2D contour slices were extracted from the 3D DNS datasets, which were pixelated to a resolution corresponding to that of the experiment. A detailed description of the code and the parameters used in the calculations is given in [16,24].

4. Image and data post processing

OH PLIF and DNS data were processed using identical post-processing algorithms, to facilitate a direct comparison of the results. The PLIF images were first corrected for a small constant background, and then segmented into burned and unburned regions, using a locally adaptive thresholding approach [25]. DNS data were segmented into burned and unburned regions along the progress variable $c = 0.5$ contour. The $c = 0.5$ contour was stored as a list of pixel coordinates to denote the flame front. The curves were then spatially smoothed by a discrete Fourier transform filter. The local curvature was calculated from the flame front coordinates using the following formula:

$$\kappa = \frac{x'y'' - y'x''}{(x'^2 + y'^2)^{\frac{3}{2}}}, \tag{1}$$

where κ is taken to be positive (negative) when the flame is convex (concave) in the direction of the unburned mixture. Both DNS and PLIF curvature data were normalised with respect to the individual box or image size. To investigate the degree of local wrinkling, the projection of the local flame normal vector a onto the flame centre reference normal vector b was evaluated at each point, using the following relation:

$$\cos\theta = \frac{a \cdot b}{|a| \cdot |b|} = \frac{a_x b_x + a_y b_y}{\sqrt{a_x^2 + a_y^2} \times \sqrt{b_x^2 + b_y^2}}. \tag{2}$$

In the case of a perfectly spherical laminar flame, the angle between the two normal vectors is zero. As the flame becomes more wrinkled, the average angle between a and b increases. For highly wrinkled flames, even negative projection angles, i.e., $\theta > 90°$, are observed.

Curvature information from the DNS data was extracted using two different approaches. For direct comparisons with PLIF data, in the first approach 2D DNS slices were extracted, pixelated, and analysed using Eq. (1).

One objective of this work was to assess to what extent curvature fields extracted from 2D measurement slices differ from the "true" curvature fields, which represent the full 3D character of the flame. For this purpose in the second approach, curvatures were evaluated using the full c-field information available from the DNS. This was done both in 2D on individual kernel slices and in 3D by taking information from adjacent kernel slices into account. For each point on the flame surface two normal vectors were calculated, the flame surface normal based on the gradient of reaction progress variable c (N_C), and the reference normal based on the position vector of the surface point (N_S):

$$N_C = -\frac{\nabla c}{|\nabla c|}, \tag{3}$$

$$N_S = \sqrt{n_x^2 + n_y^2 + n_z^2}. \tag{4}$$

The curvature was obtained by computing a tensor consisting of the gradients of the flame normal vector $h_{ij} = \partial N_{ci}/\partial x_j$ $(i = x, y, z;\ j = x, y, z)$. This tensor was then rotated into a defined local reference coordinate system, such that one of the principal directions coincided with the reference normal vector. Therefore, principal curvatures h_1 and h_2 were equal to the eigenvalues of the reduced 2D curvature tensor, and local mean curvature was defined as: $h_m = (h_1 + h_2)/2$, see [16].

In addition, the correlation between the mean curvature and the flame displacement speed S_d was investigated from the DNS data. S_d was evaluated from the reaction progress variable isosurface using:

$$S_d = \left.\frac{\dot{w} + \nabla.(\rho D \nabla c)}{\rho |\nabla c|}\right|_{c=c^*}, \tag{5}$$

where $\dot{w}$ is the chemical reaction rate; ρ is the density; D is the progress variable diffusivity; and c^* is the progress variable value defining the flame surface. It is seen from Eq. (5) that S_d depends

on local reaction-diffusion characteristic of the flame as well as local turbulence, which both affect |∇c|.

5. Results and discussion

Figure 1 shows an example of PLIF sequence obtained from the vessel at a rotor speed of 1000 rpm, for a lean ($\phi = 0.65$) CH_4/air mixture. Sharp OH gradients at the flame front of the observed flame kernels allowed easy identification and extraction of flame contour data, as the PLIF images have a high signal-to-noise ratio. This is especially important for the extraction of quantitative information, such as curvature and wrinkling, which is sensitive to noise [26]. The imaged regions shown correspond to 35 mm horizontally and 27 mm vertically. The time steps of the event shown in Fig. 1 correspond to 1.5, 4.5, 7.5, and 10.5 ms after ignition, respectively.

For OH PLIF, two CH_4/air mixtures ($\phi = 0.65$ and $\phi = 1$) corresponding to approximately unity Lewis numbers were investigated as well as a lean H_2/air mixture $\phi = 0.58$, Le < 1. For each parameter set, 30 ignition events were recorded under identical conditions on which statistics could be performed. The fact that 4 time steps were available per measurement series increased the statistical information available even further.

Figure 2 shows a 3D DNS flame kernel evolution in a turbulent environment ($Re_t = 30$). The surface plots show a progress variable value $c = 0.5$ that represents the centre region of the flame front. Clearly the effect of turbulence is evident in the form of wrinkling and increased surface area over time. The effect of decaying turbulence is also evident with small length scales evident in the initial stages that tend to smooth out over time as the turbulence decays.

Figure 3 shows flame contours and corresponding curvature pdfs from experiment and simulations. In the two left-hand columns, PLIF sequences and corresponding pdfs are shown, with corresponding DNS data shown in the two right-hand columns. The flame contours are colour coded with locations of negative curvature appearing in black and locations with positive curvature appearing in light grey. Zero curvature appears in dark grey. Note that only the last three of the available four PLIF images were used for the evaluation of curvature and wrinkling statistics due to a small number of pixels at the contour of the smallest kernels. The PLIF images correspond to $u'/S_L = 1.62$, $\phi = 1.0$ (A), $u/S_L = 5.25$, $\phi = 1.0$ (B), and $u'/S_L = 4.13$, $\phi = 0.65$ (C). The corresponding time points after ignition are indicated on the corresponding curvature pdfs. The DNS data to the right corresponds to $u'/S_L = 1.64$, $Re_t = 20$, 96^3 grid points (E), $u'/S_L = 5.1$, $Re_t = 20$, 96^3 grid points (F), and $u'/S_L = 3.8$, Re_t;= 30, 128^3 grid points (G). These values are significantly lower than at initial conditions reflecting that the turbulence decay in the DNS. u' was obtained from: $u' = [(U_{var} + V_{var} + W_{var})/3]^{1/2}$, where U_{var}, V_{var}, and W_{var} are the variances of the velocity components along the $c = 0.5$ contour. The times indicated on the pdfs are with respect to the instance when the calculation is initialised with a spherical flame kernel placed in the turbulence field. The DNS contours for the smaller simulations (96^3 grid points) are shown for 3 time steps but are seen to lie almost on top of each other. Small computational time separations are chosen

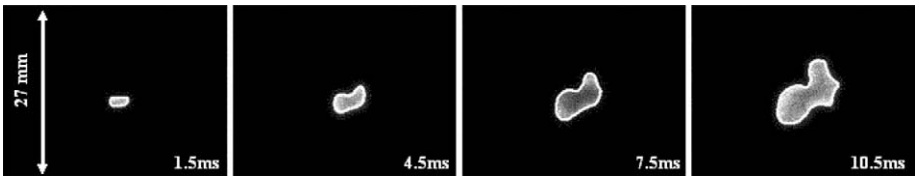

Fig. 1. Example of OH PLIF sequence capturing a single ignition event, with identified flame contour superimposed as a white outline.

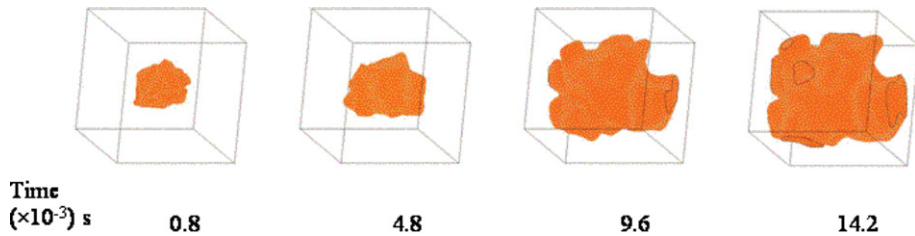

Fig. 2. Example of DNS flame kernel evolution, surface corresponding to $c = 0.5$.

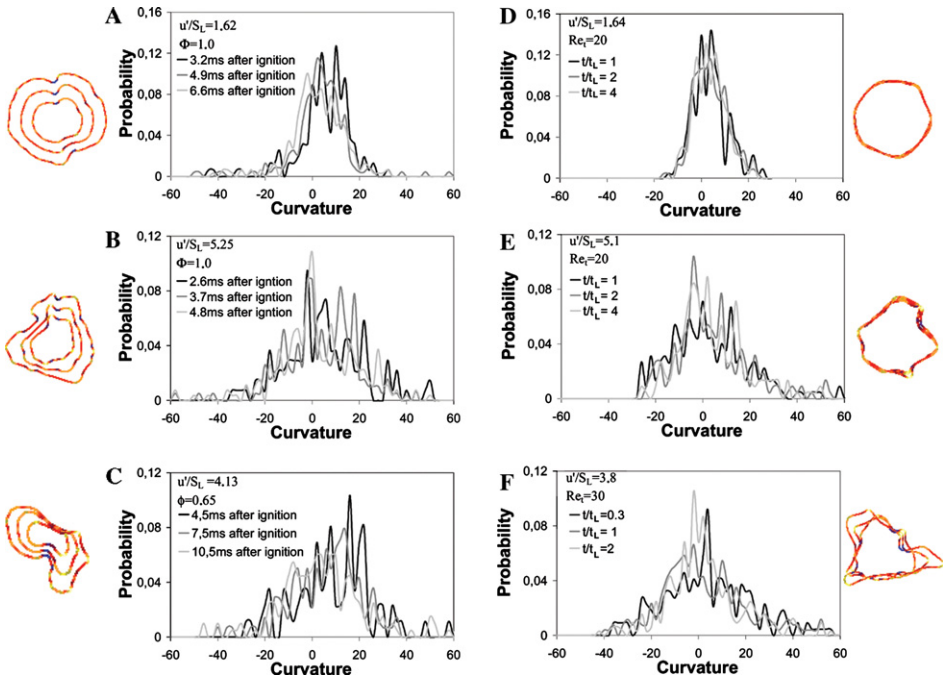

Fig. 3. Flame contour sequences and corresponding curvature pdfs: (A–C) OH PLIF CH_4/air mixture; (D–F) DNS.

in this case to mitigate effects of decaying turbulence on the kernel statistics. Note that the u'/S_L for DNS results correspond to the last event shown.

Several observations can be made: Both the response of the flame front and the development of wrinkles seem to be clearly captured by the calculations despite the simplification of the single step chemistry assumption. The spread of the pdfs is similar in both cases with mean values that are slightly positive. On both the PLIF and the DNS pdfs, it can be seen how more and more wrinkles appear as the flame kernel grows in time.

PLIF data in Fig. 3 correspond to single experimental realisations. An advantage with experiments is that statistical information is readily obtained from multiple measurements at the same time after ignition. A clearer picture of the kernel's time evolution can be obtained from averaged pdfs such as shown in Fig. 4. In Fig. 4, a averaged pdfs corresponding to different times after ignition are shown for the $u'/S_L = 1.62$, $\phi = 1.0$ case shown in Fig. 3 (columns 1 and 2, Fig. 3A). Clearly the mean curvatures are positive for all time points with mean curvatures moving closer to zero as the kernel grows (and deviates more and more from a spherical shape). Pdfs are nearly symmetric initially but become more negatively skewed with increase in time as has been previously observed [26,27]. In general, the curvature distributions change by a small amount, and the effect on the overall displacement speed S_d will be correspondingly small (see discussion later on). Figure 4B shows averaged pdfs for PLIF measurements that were performed under different turbulence intensities ($\phi = 1.0$, u'/S_L ranging from 0 to 5.25 that corresponds to rotor speeds 0, 1000, 2000, and 3000 rpm, respectively). Clearly the curvature distribution changes dramatically with increasing turbulence intensity and curvatures spread on

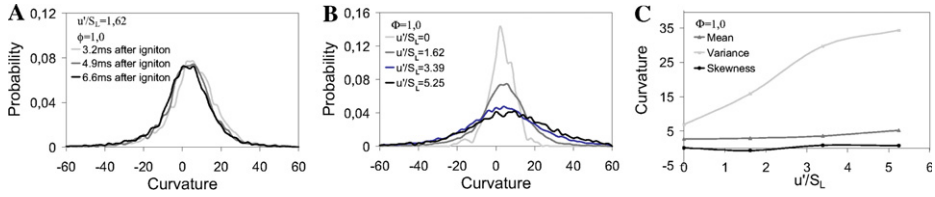

Fig. 4. OH PLIF (CH_4/air, $\varphi = 1.0$): (A) Averaged curvatures over 30 files for three different time steps after ignition at $u'/S_L = 1.62$; (B) averaged curvatures for different u'/S_L; and (C) curvature moments corresponding to data in (B).

both negative and positive sides, indicating increased wrinkling.

Curvature moments plotted in Fig. 4C, correspond to data in Fig. 4B, and show that the mean is more or less constant for different u'/S_L, with variances increasing fivefold but means remaining slightly positive for all cases. The skewness for different u'/S_L, evaluated for a fixed time, remains close to zero, indicating that the distributions remain almost symmetric all the way through. Similar observations have been made by Haq et al. [26].

Wrinkling pdfs for the cases described in Fig. 3 are shown in Fig. 5. The left-hand column corresponds to PLIF measurements in CH_4/air mixtures with $u'/S_L = 1.62$, $\phi = 1.0$ (D); $u'/S_L = 5.25$, $\phi = 1.0$ (E); and $u'/S_L = 4.13$, $\phi = 0.65$ (F). The middle column corresponds to DNS for $u'/S_L = 1.64$, $Re_t = 20$, 96^3 grid points (D); $u'/S_L = 5.1$, $Re_t = 20$, 96^3 grid points (E); and $u'/S_L = 3.8$, $Re_t = 30$, 128^3 grid points (F). The right-hand column shows PLIF data obtained from lean H_2/air mixtures (flame contours are not shown). For the latter $\phi = 0.58$, $u'/S_L = 0.41$ (G); $\phi = 0.58$, $u'/S_L = 0.87$ (H); and $\phi = 0.58$, $u'/S_L = 2.21$ (I). On all pdfs an increase in negative wrinkling is clearly apparent, increasing drastically with u'/S_L. Again, the agreement between observed and simulated pdfs is good. In the right-hand column, corresponding data for the H_2/air flame show very similar behaviour (although at much higher u' because of the higher flame speeds).

The curvature of a flame kernel is an inherently 3D property, whereas in experiments normally only the curvature in a 2D cut of the kernel can be analysed. The curvature corresponding to a slice through the $Re = 30$ DNS kernel was evaluated using both 2D and 3D c-field information, to investigate to what extent 2D curvatures differ from 3D curvatures. Pdfs of 2D and 3D curvatures shown in Fig. 6 (using the full c-field information available) are markedly different, with the pdf of the 3D curvature being nearly double as wide. This indicates that caution has to be applied when interpreting curvatures evaluated from 2D imaging data.

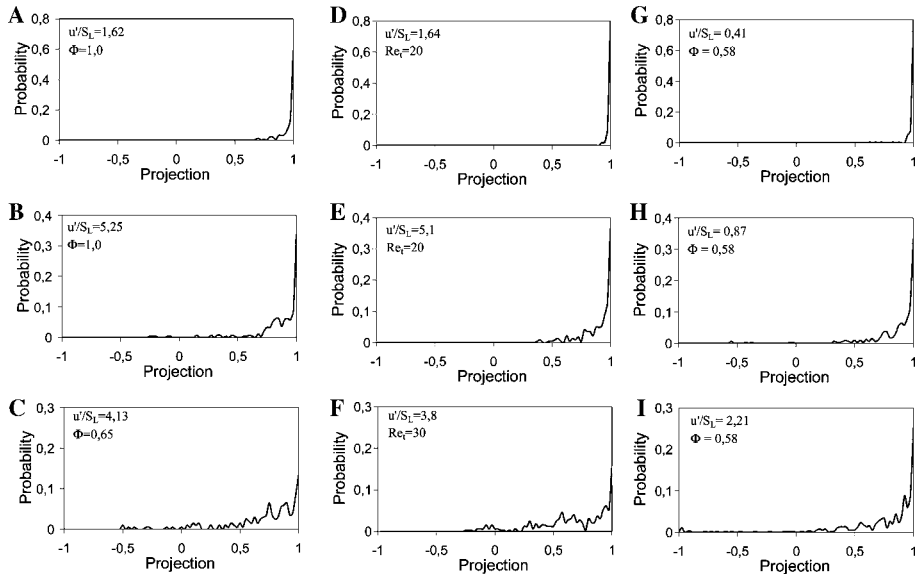

Fig. 5. Flame front wrinkling: (A–C) OH PLIF-CH_4/air; (D–F) DNS; and (G–I) OH PLIF-H_2/air.

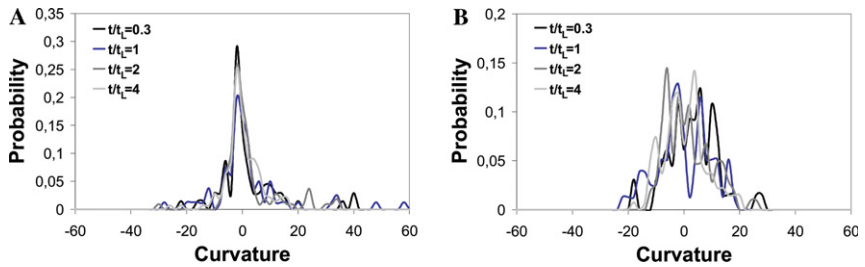

Fig. 6. (A) 2D curvature; (B) 3D curvature—of DNS data extracted using c-field information ($Re_t = 30$).

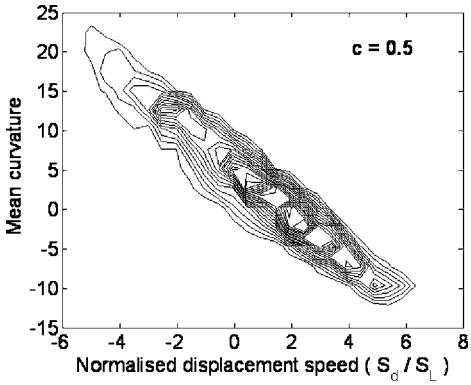

Fig. 7. Correlation between displacement speed and curvature obtained from DNS data.

Note that the 2D DNS curvature pdfs in Fig. 6A obtained from the full c-field information differ from the curvature pdfs in Fig. 3 obtained from 2D contours using pixelation method. The reason for this is that there is more spatial information on the flame front available in the continuous 2D c-field than in the truncated pixel positions used for the first approach. Another reason is that, the current filtering in the pixelation method is optimised for high spatial frequencies, and thus in low curvature regions it introduces a small artificial spread in curvature.

However, comparisons between curvatures evaluated from 2D cuts of both experimental and DNS data are still valid, if the data are extracted and analysed in the same way.

The joint pdfs of S_d and curvature are presented in Fig. 7. It is clear from the figure that displacement speed is negatively correlated with curvature, which has a strong implication in the context of flame stabilisation. This finding is consistent with previous 2D and 3D DNS results [9,28,29]. It is important to note that the displacement speed and curvature correlation are important in the context of the shape of curvature pdfs. The negatively curved isosurfaces move with higher S_d leading to flame area destruction, which ultimately reduces the probability of a finding highly negative curvature on the given c isosurface.

6. Conclusions

The effects of wrinkling on turbulent premixed flame kernels have been investigated using statistics obtained from both experiment and DNS. A comparison of the results from the two techniques shows a high level of agreement between them. This provides confidence that the simplified chemistry used in the DNS is adequate to represent the main features of the flame-turbulence interaction, and suggests that in the intermediate turbulence regime considered here, a detailed chemistry may play a subordinate role in the evolution of global flame properties. This is in contrast to previous studies focusing on very early flame propagation where chemistry may have a dominant effect [30]. At the same time, the limitations of inherently 2D measurement techniques such as PLIF can be quantified since full 3D information is available from the DNS dataset. For example, curvature pdfs constructed from 2D slices differ markedly in their statistical properties from those taking the full 3D information into account. Therefore, it is necessary to be cautious when inherent 3D flame properties are estimated from 2D measurement data such as PLIF. Within the known limitations, however, PLIF is still one of the most useful techniques to provide statistical data over a wide parameter range. This is illustrated by pdfs obtained from PLIF data of CH_4/air and H_2/air mixtures, which show markedly different behaviour attributed to the different thermo-diffusive properties of the two mixtures. The use of PLIF and DNS in combination has been demonstrated as a very powerful tool for flame analysis, with each technique compensating for the weaknesses of the other and reinforcing the strengths of both.

Acknowledgments

Support for this project in the form of a PLATFORM Grant (JREI, GR/R61994/01) from EPSRC is greatly acknowledged. This work was supported by EPSRC and Rolls-Royce plc (SG), the EC Marie Curie Fellowship programme, the Swedish Research Council, and the Swedish Energy Administration (JH), EPSRC (KWJ), the Cambridge Gates Trust (NC), and the Cambridge High Performance Computing Facility. We thank A. Dreizler, U. Maas, and S. Lindenmaier for the joint collaboration and fruitful discussion and M. Aldén for the provision of excellent experimental facilities.

References

[1] G. Damkohler, *Z. Elektrochem.* 46 (1940) 601–652, English translation as NACA Tech. Memo. No. 1112 (1947).
[2] R.S. Cant, *Phil. Trans. R. Soc. Lond. A* 357 (1999) 3583–3604.
[3] G. Searby, J. Quinard, *Combust. Flame* 73 (1990) 23–44.
[4] N. Peters, *Turbulent Combustion.* Cambridge University Press, Cambridge, UK, 2000.
[5] M. Matalon, B.J. Matkowski, *J. Fluid Mech.* 124 (1982) 239–259.
[6] N. Peters, *J. Fluid Mech.* 384 (1999) 107–132.
[7] I.G. Shepherd, R.K. Cheng, T. Plessing, C. Kortschik, N. Peters, *Proc. Combust. Inst.* 29 (2002) 1833–1840.

[8] K.W. Jenkins, R.S. Cant, *Proc. Combust. Inst.* 29 (2002) 2023–2029.
[9] N. Chakraborty, R.S. Cant, *Combust. Flame* 137 (2004) 129–147.
[10] R.G. Abdel-Gayed, D. Bradley, *Proc. Combust. Inst.* 16 (1982) 1725–1735.
[11] D. Bradley, R.A. Hicks, M. Lawes, C.G.W. Sheppard, R. Woolley, *Combust. Flame* 115 (1998) 126–144.
[12] C.F. Kaminski, J. Hult, M. Alden, S. Lindenmaier, A. Dreizler, U. Mass, M. Baum, *Proc. Combust. Inst.* 28 (2000) 399–405.
[13] M.D. Checkel, A. Thomas, *Combust. Flame* 96 (1994) 351–370.
[14] A. Dreizler, S. Lindenmaier, U. Maas, J. Hult, M. Aldén, C.F. Kaminski, *Appl. Phys. B* 70 (2000) 287–294.
[15] T. Echekki, T. Poinsot, T. Baritaud, M. Baum, in: T. Baritaud, T. Poinsot, M. Baum (Eds.), *Direct Numerical Simulation for Turbulent Reacting Flows.* Editions Technip, Paris, 1996.
[16] K.W. Jenkins, R.S. Cant, *Proc. Combust. Inst.* 29 (2002) 2023–2029.
[17] D. Thevenin, O. Gicquel, J. De Charentenay, R. Hilbert, D. Veynante, *Proc. Combust. Inst.* 29 (2002) 2031–2039.
[18] I.K. Nwagwe, H.G. Weller, G.R. Tabor, A.D. Gosman, M. Lawes, C.G.W. Sheppard, R. Woolley, *Proc. Combust. Inst.* 28 (2000) 59–65.
[19] H.G. Weller, G.R. Tabor, A.D. Gosman, C. Fureby, *Proc. Combust. Inst.* 27 (1998) 899–907.
[20] C.F. Kaminski, J. Hult, M. Aldén, *Appl. Phys. B* 68 (1999) 757–760.
[21] S. Lindenmaier, Zeitaufgelöste Laser-diagnostische Untersuchung der Funkenzündung, Ph.D. Thesis, University of Stuttgart, Stuttgart, Germany, 2001.
[22] M. Thiele, J. Warnatz, A. Dreizler, S. Lindenmaier, R. Schiessl, U. Maas, A. Grant, P. Ewart, *Combust. Flame* 128 (1–2) (2002) 74–87.
[23] T. Poinsot, T. Lele, *J. Comp. Phys.* 101–1 (1992) 104–129.
[24] K.W. Jenkins, R.S. Cant, in: D. Kinght, L. Sakell (Eds.), *Recent Advances in DNS and LES.* Kluwer Academic, New York, 1999, pp. 191–202.
[25] R. Knikker, D. Veynante, J.C. Rolon, C. Meneveau, in: *Proceedings of 10th International Symposium on Applications of Laser Techniques to Fluid Mechanics*. Lisbon, 2000.
[26] M.H. Haq, C.G.W. Sheppard, R. Woolley, D.A. Greenhalgh, R.D. Lockett, *Combust. Flame* 131 (2002) 1–15.
[27] B. Renou, A. Boukhalfa, P. Puechberty, M. Trinite, *Combust. Flame* 123 (2000) 507–521.
[28] T. Echekki, J.H. Chen, *Combust. Flame* 106 (1996) 184–202.
[29] N. Peters, P. Terhoeven, J.H. Chen, T. Echekki, *Proc. Combust. Inst.* 27 (1998) 833–839.
[30] T.J. Poinsot, Flame ignition in a premixed turbulent flow, in: *Annual Research Briefs.* Centre for Turbulent Research, Stanford Univ./NASA-Ames, Stanford, CA, 1991, pp. 251–272.

Comments

Thierry Poinsot, IMFT-CNRS Toulouse, France. DNS of flame kernels depend strongly on the initialization of the flame. How is this done here, by depositing energy or by replacing some of the fresh gases by a burned kernel? Is there turbulence inside the burned kernel at $t = 0$? How sensitive is the flame to a change in speeds for the initial turbulent velocity? Such factors would influence results.

Andreas Dreizler, TU Darmstadt, Germany. Comment to T. Poinsot's question regarding energy deposition: experimental tests have shown that varying spark energies during the arc-phase did not influence flame propagation at the times investigated in the present study.

Reply. The DNS is initialized by placing a small spherical laminar flame kernel at the center of the domain, and there is turbulence inside the kernel at $t = 0$. Naturally the early development of the kernel is influenced by the initial turbulence intensity (expressed as u'/S_L) and by the individual statistical realization of the initial turbulent velocity field, but we have not observed any significant influence on the statistics at later times. There is not experimental evidence that varying the spark energy had an influence on later flame propagation

•

Peter A.M. Kalt, University of Adelaide, Australia. The conclusion that a 2-D analysis of flame front curvature statistics from a highly wrinkled 3-D structure is not sufficient to accurately describe the flame surface is self-evident. However, the agreement between image flame curvature from PLIF and a 2-D analysis of the simulation is very good. Can you comment on the applicability, in this geometry, of a 2-plane OH-PLIF or 2-plane Rayleigh imaging in order to experimentally determine the local non-orthogonality of the flame surface with respect to the PLIF imaging plane?

Reply. One purpose of our paper is to expose what problems can occur if 2-D data are used to infer properties on inherently 3-D phenomena and to quantify such effects. If 3-D modeling is performed however, the 2-D PLIF results can always be used for quantitative comparisons by extracting image slices from the simulated results as we have shown. Of course, there are experimental techniques to recover local information on the flame front orientation in orthogonal planes to the laser sheet, one of which is sweeping the laser sheet across the volume of interest [1] or, indeed using a double sheet technique as the author suggests. All these techniques are limited in their resolution, however, and the complexity of their approach may not justify the limited extra gradient information that is afforded in this way.

Reference

[1] Hult, et al., *Exp. Fluids* 33 (2002) 265–269.

•

Friedrich Dinkellacker, University of Erlangen, Germany. First, I appreciate the approach to evaluate both the experimental and the DNS data with the same procedure and software. You showed the relation between mean curvature and normalized displacement speed. What is meant by "mean" curvature here; the average of what? Did you correlate between instantaneous curvature and displacement speed?

Reply. The mean curvature is the arithmetic mean of two principal curvatures on a given point of a given surface. The principal curvatures (κ_1 and κ_2) are given by two non-zero eigenvalues of the matrix $\partial N_i/\partial x_j$. From the properties of the second-order tensor $\partial N_i/\partial x_j$, the mean curvature is given by: $\kappa_m = (\kappa_1 + \kappa_1)/2 = (\partial N_i/\partial x_j)/2$. Thus, in Fig. 7 of the paper, the correlation between instantaneous mean curvature and displacement speed is presented.

•

Ravi Sangras, American Air Liquide, USA. Does the flame have a positive curvature in general? More of a suggestion—have you tried correlating the curvature with $\wedge_l$, S_L, μ_l, etc. as in Chen and Bilger [1]—you might see some correlations.

Reference

[1] Y.C. Chen, R.W. Bilger, *Proc. Combust. Inst.* 30 (2005) 801–808.

Reply. Curvature pdfs obtained from both experiment and simulations are slightly shifted towards positive values. As the flame kernels are expanding outwards, a positively biased curvature pdf is expected.

The suggestions on curvature correlations are interesting, and we are looking forward to see the publication that the reviewer refers to. We are already undertaking work along these lines.